

## ON VARIATIONS IN THE PEAK LUMINOSITY OF TYPE IA SUPERNOVAE

F. X. TIMMES<sup>1</sup>, EDWARD F. BROWN<sup>2</sup>, J. W. TRURAN<sup>1,2</sup>

Center for Astrophysical Thermonuclear Flashes, The University of Chicago, Chicago, IL 60637

To appear in THE ASTROPHYSICAL JOURNAL LETTERS

### ABSTRACT

We explore the idea that the observed variations in the peak luminosities of Type Ia supernovae originate in part from a scatter in metallicity of the main-sequence stars that become white dwarfs. Previous, numerical, studies have not self-consistently explored metallicities greater than solar. One-dimensional Chandrasekhar mass models of SNe Ia produce most of their <sup>56</sup>Ni in a burn to nuclear statistical equilibrium between the mass shells  $0.2M_{\odot}$  and  $0.8M_{\odot}$ , for which the electron to nucleon ratio  $Y_e$  is constant during the burn. We show analytically that, under these conditions, charge and mass conservation constrain the mass of <sup>56</sup>Ni produced to depend *linearly* on the original metallicity of the white dwarf progenitor. Detailed post-processing of W7-like models confirms this linear dependence. The effect that we have identified is most evident at metallicities larger than solar, and is in agreement with previous self-consistent calculations over the metallicity range common to both calculations. The observed scatter in the metallicity ( $\frac{1}{3}Z_{\odot}$ – $3Z_{\odot}$ ) of the solar neighborhood is enough to induce a 25% variation in the mass of <sup>56</sup>Ni ejected by Type Ia supernova. This is sufficient to vary the peak *V*-band brightness by  $|\Delta M_V| \approx 0.2$ . This scatter in metallicity is present out to the limiting redshifts of current observations ( $z \lesssim 1$ ). Sedimentation of <sup>22</sup>Ne can possibly amplify the variation in <sup>56</sup>Ni mass to  $\lesssim 50\%$ . Further numerical studies can determine if other metallicity-induced effects, such as a change in the mass of the <sup>56</sup>Ni-producing region, offset or enhance the variation we identify.

*Subject headings:* nuclear reactions, nucleosynthesis, abundances — stars: abundances — supernovae: general — galaxies: abundances — galaxies: evolution

### 1. INTRODUCTION

The maximum luminosity of Type Ia supernovae (SNe Ia) is a key ingredient of their analysis and is also essential for their use as distance indicators in cosmology (Fillipenko 1997; Branch 1998; Leibundgut 2001). For the nearby SNe Ia with Cepheid-determined distances, the overall dispersion in the peak magnitude measurements is rather small, about 0.5 mag. in *B* and *V* (Fillipenko 1997; Saha et al. (1999); Gibson et al. 2000). When the sample is enlarged to include more distant SNe Ia, there are several subluminous events that broaden the variation to about 1 mag. in *B* (Hamuy et al. 1996; Riess et al. 1998; Perlmutter et al. 1999; Phillips et al. 1999), but the bulk of the SNe Ia sample have peak brightnesses within a 0.5 mag. range in *B* and *V*.

An interesting feature of SNe Ia is that the luminosity is set not by the explosion, for which the deposited energy goes into expansion, but rather by the decay of <sup>56</sup>Ni and <sup>56</sup>Co that are formed during the nucleosynthesis (Arnett 1982; Pinto & Eastman 2000). At the time of peak luminosity, <sup>56</sup>Co has not yet decayed, and hence the peak luminosity is a measurement of the amount of <sup>56</sup>Ni synthesized during the explosion. This amount presumably depends on the progenitor and on the details of the explosion. In particular, it has long been known that the amount of <sup>56</sup>Ni synthesized depends in part on the asymmetry between neutrons and protons in the progenitor white dwarf (Truran, Arnett, & Cameron 1967; Arnett, Truran, & Woosley 1971).

In this Letter we explore how the intrinsic variation in the initial CNO abundances of the progenitors translates into a variation in the mass of <sup>56</sup>Ni synthesized ( $M(^{56}\text{Ni})$ ) and hence

in the peak luminosity of SNe Ia. We show analytically, using mass and charge conservation, that  $M(^{56}\text{Ni})$  depends *linearly* on the initial metallicity  $Z$ , and that the observed variation in the  $Z$  of field dwarfs, from  $\frac{1}{3}$  to 3 times solar, leads to a  $\approx 25\%$  variation in  $M(^{56}\text{Ni})$ , with most of the effect occurring at  $Z > Z_{\odot}$ . This is the expected variation if SNe Ia progenitors uniformly represent the range of CNO abundances observed in stars today. Our conclusion rests on (1) considerations of nuclear equilibrium during the explosion, and (2) the observed scatter in  $Z$  of stars within the Galactic disk.

The dependence of the ejected <sup>56</sup>Ni mass on the progenitor's initial  $Z$  has been investigated previously, both via the evolution of the progenitor (Umeda et al. 1999a; Umeda et al. 1999b; Domínguez, Höflich, & Straniero 2001, hereafter D01) and the explosion itself (Höflich, Wheeler, & Thielemann 1998; Iwamoto et al. 1999; D01). Although these one-dimensional simulations are sophisticated in their treatment of the flame microphysics and the nuclear burning, we desire to elucidate features that are robust to any complicated hydrodynamics. Our demonstration that the mass of nickel depends linearly on the initial  $Z$  of the progenitor serves as a check and stimulus for future numerical studies and provides insight into possible evolutionary effects.

In § 2 we demonstrate the linear dependence of  $M(^{56}\text{Ni})$  on the progenitor's  $Z$ , and compare this with detailed nucleosynthesis calculations and previous numerical work. We speculate on the source of differences between different calculations, and then discuss the intrinsic scatter in CNO abundances in the ISM (§ 3) and the implications (§ 4) of our results.

Electronic address: fxt@flash.uchicago.edu

<sup>1</sup> Dept. of Astronomy & Astrophysics, The University of Chicago, Chicago, IL 60637

<sup>2</sup> Enrico Fermi Institute, The University of Chicago, Chicago, IL 60637

Nearly all one-dimensional Chandrasekhar mass models of SNe Ia produce most of their  $^{56}\text{Ni}$  in a burn to nuclear statistical equilibrium (NSE) between the mass shells  $0.2M_\odot$  and  $0.8M_\odot$  (Nomoto, Thielemann, & Yokoi 1984; Höflich et al. 1998; Iwamoto et al. 1999; Höflich et al. 2000). In this region, unlike in the innermost  $0.2M_\odot$  (Brachwitz et al. 2000), weak interactions operate on timescales longer than the time for the thermonuclear burning front to disrupt the white dwarf. Following this rapid burn to NSE, most of the mass is in the iron-peak nuclei  $^{56}\text{Ni}$ ,  $^{58}\text{Ni}$ , and  $^{54}\text{Fe}$ . First consider the case when  $^{56}\text{Ni}$  and  $^{58}\text{Ni}$  are the only two competing species. The addition of  $^{54}\text{Fe}$  will be considered next. Mass and charge conservation,

$$\sum_{i=1}^n X_i = 1, \quad \sum_{i=1}^n \frac{Z_i}{A_i} X_i = Y_e \quad (1)$$

imply that the mass fraction of  $^{56}\text{Ni}$  depends linearly on  $Y_e$ ,

$$X(^{56}\text{Ni}) = 58Y_e - 28, \quad (2)$$

where isotope  $i$  has  $Z_i$  protons,  $A_i$  nucleons (protons + neutrons), and a mass fraction  $X_i$ . The aggregate ensemble has a proton to nucleon ratio of  $Y_e$ .

Most of a main-sequence star's initial  $Z$  comes from the CNO and  $^{56}\text{Fe}$  nuclei inherited from its ambient interstellar medium. The slowest step in the hydrogen burning CNO cycle is proton capture onto  $^{14}\text{N}$ . This results in all the CNO catalysts piling up into  $^{14}\text{N}$  when hydrogen burning on the main sequence is completed. During helium burning the reactions  $^{14}\text{N}(\alpha, \gamma)^{18}\text{F}(\beta^+, \nu_e)^{18}\text{O}(\alpha, \gamma)^{22}\text{Ne}$  convert all of the  $^{14}\text{N}$  into  $^{22}\text{Ne}$ . Thus, the mass fraction of  $^{22}\text{Ne}$  in the carbon-oxygen white dwarf remnant is

$$X(^{22}\text{Ne}) = 22 \left( \frac{X(^{12}\text{C})}{12} + \frac{X(^{14}\text{N})}{14} + \frac{X(^{16}\text{O})}{16} \right), \quad (3)$$

where the mass fractions refer to the original distribution of the star (prior to main-sequence burning). For a uniform distribution of  $^{22}\text{Ne}$  and  $^{56}\text{Fe}$  throughout the star, eq. (1) gives the initial  $Y_e$  of the white dwarf

$$Y_e = \frac{10}{22} X(^{22}\text{Ne}) + \frac{26}{56} X(^{56}\text{Fe}) + \frac{1}{2} [1 - X(^{22}\text{Ne}) - X(^{56}\text{Fe})]. \quad (4)$$

According to the argument at the beginning of this section, this  $Y_e$  is fixed in the region where the  $^{56}\text{Ni}$  is created. Substituting eqs. (4) and (3) into eq. (2) leads to a linear expression for the mass fraction of  $^{56}\text{Ni}$  in an NSE distribution in terms of the main-sequence star's initial  $Z$

$$\begin{aligned} X(^{56}\text{Ni}) &= 1 - 58 \left[ \frac{X(^{12}\text{C})}{12} + \frac{X(^{14}\text{N})}{14} + \frac{X(^{16}\text{O})}{16} + \frac{X(^{56}\text{Fe})}{28} \right] \\ &= 1 - 0.057 \frac{Z}{Z_\odot}. \end{aligned} \quad (5)$$

The average peak  $B$  and  $V$  magnitudes of nearby SNe Ia (Gibson et al. 2000; Saha et al. 1999) strongly imply that a fiducial SNe Ia produces  $\approx 0.6M_\odot$  of  $^{56}\text{Ni}$ . Taking eq. (5) to represent the mass fraction of  $^{56}\text{Ni}$  relative to this fiducial mass gives

$$M(^{56}\text{Ni}) \approx 0.6M_\odot \left( 1 - 0.057 \frac{Z}{Z_\odot} \right). \quad (6)$$

Here we assume that  $Y_e$  is uniform throughout the star, and that all material within the  $^{56}\text{Ni}$ -producing mass shell passes through NSE with normal freeze-out.

If  $^{54}\text{Fe}$  is also present then an additional Saha-like equation for the chemical potentials (Clifford & Tayler 1965) is required. Consider the chemical equation  $\alpha^{56}\text{Ni} + \beta^{54}\text{Fe} \leftrightarrow \gamma^{58}\text{Ni}$ . Both  $^{54}\text{Fe}$  and  $^{58}\text{Ni}$  carry two extra neutrons; this fixes the stoichiometric ratios  $\gamma/\beta = 1$  and  $\beta/\alpha = 14$ . As a result, the equation for chemical equilibrium is of the form  $X(^{54}\text{Fe})/X(^{58}\text{Ni}) = [f(T, \rho)/X(^{56}\text{Ni})]^{1/14}$ . Here  $f(T, \rho)$  contains the mass excesses and phase space factors common to the chemical potential of the three species. Expanding about  $T = 5 \times 10^9 \text{ K}$ ,  $\rho = 10^8 \text{ g cm}^{-3}$ , and  $X(^{56}\text{Ni}) = 1.0$ , we find that

$$\begin{aligned} \frac{X(^{54}\text{Fe})}{X(^{58}\text{Ni})} &\approx 2.1 \left( \frac{T}{5 \times 10^9 \text{ K}} \right)^{0.4} \left( \frac{\rho}{10^8 \text{ g cm}^{-3}} \right)^{-0.07} \\ &\quad \times X(^{56}\text{Ni})^{-0.07}. \end{aligned} \quad (7)$$

For this ratio,  $X(^{54}\text{Fe})/X(^{58}\text{Ni}) \approx 2$ , the relationship between  $Z$  and  $X(^{56}\text{Ni})$  becomes slightly shallower than eq. (5),  $X(^{56}\text{Ni}) = 1 - 0.054(Z/Z_\odot)$ . Similar considerations show that  $^{56}\text{Fe}$  is not present unless  $Y_e$  is much smaller than the case considered. Equation (7) does not hold if an alpha-rich freeze-out occurs, in which case  $(\alpha, \gamma)$  reactions convert  $^{54}\text{Fe}$  to  $^{58}\text{Ni}$ . Hence the ratio  $X(^{58}\text{Ni})/X(^{54}\text{Fe})$  is sensitive to the flame speed. The  $^{56}\text{Ni}$  mass is affected only slightly, however, as the charge-to-mass of  $^{58}\text{Ni}$  (which sets the slope in eq. [2]) is  $28/58 = 0.483$  and differs by only 0.3% from the charge-to-mass of  $^{54}\text{Fe}$ ,  $26/54 = 0.481$ . Our main result, eq. (5), is thus relatively insensitive to the precise details of the explosion, so long as NSE favors a  $^{56}\text{Ni}$ -dominated ‘‘iron’’ peak.

The simple linear relation between  $Y_e$  and the mass fraction of  $^{56}\text{Ni}$  in eq. (5) is robust, as it only relies on basic properties of NSE. As a test of this analytical result, we calculated the mass of  $^{56}\text{Ni}$  ejected by W7-like models (Nomoto et al. 1984; Thielemann, Nomoto, & Yokoi 1986; Iwamoto et al. 1999) by integrating a 510 isotope nuclear reaction network over the thermodynamical trajectories for a wide range of  $Z$ . The results are shown in Fig. 1 with the short-dashed curve. We also plot the linear relation (eq. [6]; *solid curve*), with  $Z/Z_\odot$  adjusted to give the  $^{22}\text{Ne}$  abundance used by W7,  $X(^{22}\text{Ne}) = 0.025Z/Z_\odot$ . Most of the differences between eq. (6) and the detailed W7-like models is attributable to our assumption that all of the  $^{56}\text{Ni}$  comes from the 0.2 to  $0.8M_\odot$  region in the white dwarf, with an additional small correction for our neglect of weak interactions that slightly decrease  $Y_e$ . The difference between the slope given by the detailed W7-like models and the analytical model is less than 5%.

Previous investigations (Höflich et al. 1998; D01) into the effect of a varying  $X(^{22}\text{Ne})$  do not agree on the mass of  $^{56}\text{Ni}$  produced. Höflich et al. (1998) found that varying the metallicity from  $Z = 0.1Z_\odot$  to  $Z = 10Z_\odot$  produced only an  $\approx 4\%$  variation in the  $^{56}\text{Ni}$  mass ejected, in sharp contrast to our results as well the results of Iwamoto et al. (1999), who found that increasing  $Z$  from zero to solar in fast-deflagration models leads to an  $\approx 10\%$  decrease in the  $^{56}\text{Ni}$  mass ejected. Both of these works relied on post-processing the thermodynamical trajectories, as we have done. Recently, D01 investigated the range  $10^{-10}Z_\odot$  to  $0.02Z_\odot$ . Of the one-dimensional calculations just mentioned, only this one accounts for the effect of  $Y_e$  on the energy generation rate. The long-dashed curve in Fig. 1 shows the D01 results for their  $1.5M_\odot$  progenitors; other progenitor masses in their survey display the same trend with  $Z$ . Our analytical result and post-processed W7-like models essentially agree with the findings of D01 over the range of metallicities common to all three calculations. As is evident in Fig. 1, the largest variation in the mass of  $^{56}\text{Ni}$  occurs at

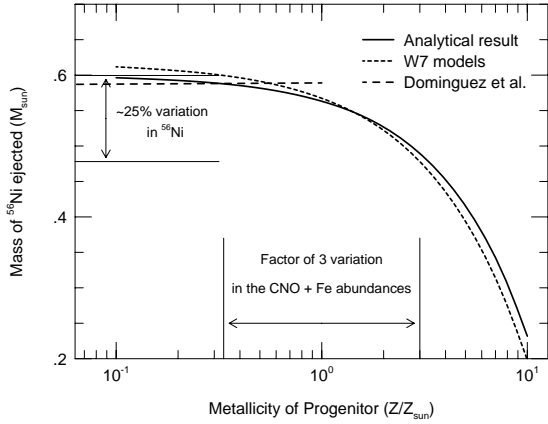


FIG. 1.— Mass of  $^{56}\text{Ni}$  ejected by SNe Ia as a function of the initial metallicity  $Z$ . Shown is the linear relation (*solid curve*; the curvature is from the logarithmic abscissa) of eq. (6) for  $X(^{22}\text{Ne}) = 0.024(Z/Z_{\odot})$ , a sequence of W7-like models (*short-dashed curve*), and the calculation of D01 for  $1.5 M_{\odot}$  progenitors (*long-dashed curve*). Other progenitor masses in the D01 survey display the same trend with  $Z$ . As indicated by the arrows, a scatter of 3 about the mean in  $Z$  of the main-sequence stars that produce white dwarfs leads to a variation of about 25% ( $0.13 M_{\odot}$ ) of  $^{56}\text{Ni}$  ejected if the metals are uniformly distributed within the white dwarf. A factor of seven scatter about the mean in the initial metallicity corresponds to a factor of 2 variation in  $M(^{56}\text{Ni})$ .

$Z > Z_{\odot}$ . We note that the calculations of D01 evolve a main-sequence star into the SNe Ia progenitor, whereas our calculation and those of Iwamoto et al. (1999) start from a given white dwarf configuration.

As a caveat, we note that our post-processing of the W7 thermodynamic trajectories is not completely self-consistent. The reason is that the temperature and density profiles of the W7 were calculated using the energy released by burning matter of solar  $Z$ . While  $Z$  is likely to influence the flame propagation (via the change in the rate of energy production; Hix & Thielemann 1996, 1999), in the mass range under consideration Si-burning is complete, so our assumption of NSE still holds. Indeed, Domínguez & Höflich (2000) found that the mass of  $^{56}\text{Ni}$  synthesized was also rather insensitive to the details of the flame microphysics. It is also possible the density,  $\rho_{\text{tr}}$ , at which a transition from deflagration to detonation occurs will influence the amount of  $^{56}\text{Ni}$  produced (Höflich, Khokhlov, & Wheeler 1995, and references therein). Fits to observations seem to require, however, that  $\rho_{\text{tr}} \approx 10^7 \text{ g cm}^{-3}$  which corresponds to a Lagrangian mass coordinate of  $\sim 1.0 M_{\odot}$ , which is exterior to the main  $^{56}\text{Ni}$ -producing layers. Further numerical studies should elucidate the source of the discrepancy. In particular they should determine if other effects, such as a systematic change in the mass coordinates where most of the  $^{56}\text{Ni}$  is produced, offsets or enhances the variation in  $M(^{56}\text{Ni})$  that we find. The demonstrated linear dependence between  $M(^{56}\text{Ni})$  and  $Z$  will make it easier to untangle competing physical effects in a fully self-consistent calculation.

### 3. SCATTER IN THE INITIAL METALLICITY AND THE INDUCED BRIGHTNESS VARIATIONS

Stellar abundance determinations are discussed in terms of an elemental abundance relative to iron,  $[X/\text{Fe}]$ , as a function of the iron to hydrogen ratio  $[\text{Fe}/\text{H}]$ , primarily because  $[\text{Fe}/\text{H}]$  is relatively easy to measure in stars. The  $[\text{Fe}/\text{H}]$  ratio represents a chronometer in that the accumu-

lation of iron in the ISM increases monotonically with time (Wheeler, Sneden, & Truran 1989). Calibration of  $[\text{Fe}/\text{H}]$  as a function of time forms the basis of the age-metallicity relationship.

The  $Z$  of local field stars rapidly increased about 10–13 Gyr ago during formation of the Galaxy’s disk and then increased much more gradually over the last  $\sim 10$  Gyr (Twarog 1980; Edvardsson et al. 1993; Feltzing, Holmberg, & Hurley 2001). More importantly for our purposes, however, is the relatively large scatter in stellar metallicities,  $\Delta[\text{Fe}/\text{H}] \sim 0.5$ , at any given age. Feltzing et al. (2001) constructed an age-metallicity diagram for 5828 dwarf and sub-dwarf stars from the Hipparcos Catalog using evolutionary tracks to derive ages and Strömgren photometry to derive metallicities. They concluded that the age-metallicity diagram is well-populated at all ages, that old, metal-rich stars do exist, and that the scatter in  $Z$  at any given age is larger than the observational errors. Other surveys of stellar metallicities (Edvardsson et al. 1993; Chen et al. 2000) are in good agreement with these trends.

The most abundant elements in the Galaxy after H and He are CNO. Both  $[\text{C}/\text{Fe}]$  and  $[\text{N}/\text{Fe}]$  in halo and disk dwarfs are observed to be roughly solar and constant (Laird 1985; Carbon et al. (1987); Wheeler et al. (1989)). The  $[\text{O}/\text{Fe}]$  ratio is larger at low metallicities—oxygen being the dominant element ejected by SNe II—and then slowly decreases due to variations in mass and  $Z$  (Gratton 1985; Peterson, Kurucz, & Carney 1990; Timmes, Woosley, & Weaver 1995). Within these general trends is a relatively large scatter,  $\Delta[\text{C}/\text{Fe}] \sim \Delta[\text{N}/\text{Fe}] \sim \Delta[\text{O}/\text{Fe}] \sim 0.5$  dex, at any given  $[\text{Fe}/\text{H}]$ .

According to the simple analytical relation (eq. [5]) and the detailed W7-like models (Fig. 1), a scatter of a factor of 3 about the mean in the initial metallicity ( $\frac{1}{3}Z_{\odot} < Z < 3Z_{\odot}$ ) leads to a variation of about 25% ( $0.13 M_{\odot}$ ) in the mass of  $^{56}\text{Ni}$  ejected by SNe Ia if the  $^{22}\text{Ne}$  and  $^{56}\text{Fe}$  are uniformly distributed within the white dwarf. The minimum peak brightness variations caused by this variation in  $^{56}\text{Ni}$  mass are  $|\Delta M_V| \approx 0.2$  (Pinto & Eastman 2001). Thus, the amplitude of this effect cannot account for all of the observed variation in peak luminosity of local SNe Ia (0.5 magnitude in  $B$  and  $V$ ). The observed scatter in peak brightnesses may be even larger, as Cepheid-based distances to the host galaxies of peculiar events such as sub-luminous SN 1991bg or brighter-than-normal SN 1991T haven’t been measured yet (Saha et al. 1999; Contardo, Leibundgut, & Vacca 2000; Leibundgut 2000). There is evidence for a larger scatter when more distant supernovae are included (Hamuy et al. 1996; Riess et al. 1998). It would take a scatter of about a factor of seven ( $\Delta[\text{Fe}/\text{H}] \sim 0.8$  dex) in the initial  $Z$  to account for a factor of two variation in the  $^{56}\text{Ni}$  mass and peak luminosity.

### 4. IMPLICATIONS AND SUMMARY

Using the properties of NSE, we find that where weak interactions are unimportant the mass fraction of  $^{56}\text{Ni}$  produced depends linearly upon the initial metallicity of the white dwarf progenitor. This result is robust: so long as the region that reaches NSE does so on a timescale over which  $Y_e$  is nearly constant, then the mass of  $^{56}\text{Ni}$  produced is largely independent of the detailed physics of the flame front propagation. This fact offers a check on sophisticated numerical calculations and could be exploited to understand better the disagreements between different codes.

The variation from  $\frac{1}{3}$  to 3 times solar metallicity observed in dwarf stars in the Galactic disk implies that SNe Ia should

have a minimum variation of 25% in the ejected  $^{56}\text{Ni}$  mass. This has implications for the brightness variations observed in both near and distant SNe Ia and for galactic chemical evolution. The most distant SNe Ia observed today have redshifts  $z \lesssim 1$ . This corresponds to a lookback time of about 4–7 Gyr depending on the cosmological model, and implies a mean  $[\text{Fe}/\text{H}]$  ratio between -0.1 and -0.3. There is, however, still a scatter of  $\Delta[\text{Fe}/\text{H}] \sim 0.5$  at these mean  $[\text{Fe}/\text{H}]$  ratios (see the discussion in § 3). We therefore expect that the variation in peak luminosities of SNe Ia in spiral galaxies at  $z \lesssim 1$  will show the same minimum variation of  $|\Delta M_V| \approx 0.2$  in peak luminosity as nearby SNe Ia. This variation is superposed on other evolutionary effects, such as that from a reduction in the C/O ratio (Höflich et al. 1998; D01).

For combustion to NSE with no freeze-out (see § 2), the  $^{56}\text{Ni}$  mass is anticorrelated with the mass of  $^{54}\text{Fe}$  and  $^{58}\text{Ni}$  ejected, and subluminal SNe Ia will tend, therefore, to have larger  $^{54}\text{Fe}/^{56}\text{Fe}$  ratios than brighter ones. Because SNe Ia produce  $> \frac{1}{2}$  of the galactic iron-peak nuclei<sup>3</sup>, the isotopic ratios among the iron group in SNe Ia ejecta should not exceed the solar ratios by about a factor of two (Iwamoto et al. 1999; Wheeler et al. 1989). There are several uncertainties with the  $^{54}\text{Fe}/^{56}\text{Fe}$  ratio. First, some of the  $^{54}\text{Fe}$  is produced in the core where weak interactions are important for determining the final  $Y_e$  (although this may be alleviated by the overturning of matter in the core from Rayleigh-Taylor instabilities; see Gamezo et al. 2003 for a recent calculation). At high densities these reaction rates are sensitive to the input nuclear physics (Brachwitz et al. 2000; Martínez-Pinedo, Langanke, & Dean 2000). Isotopic measurements of cosmic rays, such as with *Ulysses* (Connell & Simpson 1997; Connell 2001) and *ACE* (Wiedenbeck et al. 2001) can probe the evolution of  $^{54}\text{Fe}/^{56}\text{Fe}$  over the past  $\approx 5$  Gyr.

Since most of the  $^{56}\text{Ni}$  created in one-dimensional SNe Ia models lies in the  $0.2M_\odot$ – $0.8M_\odot$  mass shell, our assumption of a uniform  $^{22}\text{Ne}$  distribution deserves close scrutiny. There has long been speculation about sedimentation of  $^{22}\text{Ne}$  and its effect on the cooling of isolated white dwarfs (Bildsten & Hall 2001; Deloye & Bildsten 2002; Hansen et al. 2002, and references therein). If, for example, all of the  $^{22}\text{Ne}$  from the outermost  $0.6M_\odot$  were to settle into the shell between  $0.2M_\odot$  and  $0.8M_\odot$ , then the effective  $Y_e$  in this shell would double. Indeed, Bildsten & Hall (2001) noted that the production of  $^{54}\text{Fe}$  was an indirect test of the sedimentation of  $^{22}\text{Ne}$ . For nearby SNe Ia, which presumably sample a range of progenitor ages, the variability in  $^{56}\text{Ni}$  production would increase to 50%, or about  $\Delta M_V \approx 0.3$ . Since it takes about 7 Gyr for  $^{22}\text{Ne}$  at the surface to fall through the outer  $\approx 0.4M_\odot$  of a  $1.2M_\odot$  CO white dwarf (Bildsten & Hall 2001), the effect of sedimentation will be diminished for those SNe Ia at  $z \approx 1$ .

We thank Franziska Brachwitz and Friedel Thielemann for providing the initial W7 thermodynamic trajectories. We also thank the referees for their critical reading, which greatly improved the manuscript. This work is supported by the Department of Energy under Grant No. B341495 to the Center for Astrophysical Thermonuclear Flashes and Grant No. DE-FG02-91ER40606 in Nuclear Physics and Astrophysics at the University of Chicago.

<sup>3</sup> SNe Ia produce  $\approx 0.8M_\odot$  of iron-group nuclei while Type II SNe produce  $\approx 0.1M_\odot$ , and the ratio of thermonuclear to core collapse events is about 0.15–0.27 in the Galaxy (van den Bergh & Tammann 1991; Cappellaro et al. 1997).

#### REFERENCES

- Arnett, W. D. 1982, *ApJ*, 253, 785  
 Arnett, W. D., Truran, J. W., & Woosley, S. E. 1971, *ApJ*, 165, 87  
 van den Bergh, S. & Tammann, G. A. 1991, *ARA&A*, 29, 363  
 Bildsten, L. & Hall, D. 2001, *ApJ*, 549, L219  
 Brachwitz, F. et al. 2000, *ApJ*, 536, 934  
 Branch, D. 1998, *ARA&A*, 36, 17  
 Cappellaro, E., Turatto, M., Tsvetkov, D. Y., Bartunov, O. S., Pollas, C., Evans, R., & Hamuy, M. 1997, *A&A*, 322, 431  
 Carbon, D. F., Barbuy, B., Kraft, R. P., Friel, E. D., & Suntzeff, N. B. 1987, *PASP*, 99, 335  
 Chen, Y. Q., Nissen, P. E., Zhao, G., Zhang, H. W., & Benoni, T. 2000, *A&AS*, 141, 491  
 Clifford, F. E., & Tayler, R. F. 1965, *MNRAS*, 129, 104  
 Connell, J. J. 2001, *Space Sci. Rev.*, 99, 41  
 Connell, J. J., & Simpson, J. A. 1997, *ApJ*, 475, L61  
 Contardo, G., Leibundgut, B., & Vacca, W. D. 2000, *A&A*, 359, 876  
 Deloye, C. J. & Bildsten, L. 2002, *ApJ*, 580, 1077  
 Domínguez, I. & Höflich, P. 2000, *ApJ*, 528, 854  
 Domínguez, I., Höflich, P., & Straniero, O. 2001, *ApJ*, 557, 279 (D01)  
 Edvardsson, B., Andersen, J., Gustafsson, B., Lambert, D. L., Nissen, P. E., & Tomkin, J. 1993, *A&A*, 275, 101  
 Feltzing, S., Holmberg, J., & Hurley, J. R. 2001, *A&A*, 377, 911  
 Fillipenko, A. V. 1997, *ARA&A*, 35, 309  
 Gamezo, V. N., Khokhlov, A. M., Oran, E. S., Chtchelkanova, A. Y., & Rosenberg, R. O. 2003, *Science*, 299, 77  
 Gibson, B. K. et al. 2000, *ApJ*, 529, 723  
 Gratton, R. G. 1985, *A&A*, 148, 105  
 Hamuy, M., Phillips, M. M., Suntzeff, N. B., Schommer, R. A., Maza, J., Smith, R. C., Lira, P., & Aviles, R. 1996, *AJ*, 112, 2438  
 Hansen, B. M. S. et al. 2002, *ApJ*, 574, L155  
 Hix, W. R., & Thielemann, F.-K. 1996, *ApJ*, 460, 869  
 Hix, W. R., & Thielemann, F.-K. 1999, *ApJ*, 511, 862  
 Höflich, P., Khokhlov, A. M., & Wheeler, J. C. 1995, *ApJ*, 444, 831  
 Höflich, P., Wheeler, J. C., & Thielemann, F. K. 1998, *ApJ*, 495, 617  
 Höflich, P., Nomoto, K., Umeda, H., & Wheeler, J. C. 2000, *ApJ*, 528, 590  
 Iwamoto, K., Brachwitz, F., Nomoto, K., Kishimoto, N., Umeda, H., Hix, W. R., & Thielemann, F. 1999, *ApJS*, 125, 439  
 Laird, J. B. 1985, *ApJ*, 289, 556  
 Leibundgut, B. 2000, *A&A rev.*, 10, 179  
 Leibundgut, B. 2001, *ARA&A*, 39, 67  
 Martínez-Pinedo, G., Langanke, K., & Dean, D. J. 2000, *ApJS*, 126, 493  
 Nomoto, K., Thielemann, F.-K., & Yokoi, K. 1984, *ApJ*, 286, 644  
 Perlmutter, S., et al. 1999, *ApJ*, 517, 565  
 Peterson, R. C., Kurucz, R. L., & Carney, B. W. 1990, *ApJ*, 350, 173  
 Pinto, P. A. & Eastman, R. G. 2000, *ApJ*, 530, 744  
 Pinto, P. A. & Eastman, R. G. 2001, *New Astronomy*, 6, 307  
 Phillips, M. M., Lira, P., Suntzeff, N. B., Schommer, R. A., Hamuy, M., Maza, J., *AJ*, 118, 1766  
 Riess, A. G. et al. 1998, *AJ*, 116, 1009  
 Saha, A., Sandage, A., Tammann, G. A., Labhardt, L., Macchetto, F. D., & Panagia, N. 1999, *ApJ*, 522, 802  
 Thielemann, F.-K., Nomoto, K., & Yokoi, K. 1986, *A&A*, 158, 17  
 Timmes, F. X., Woosley, S. E., & Weaver, T. A. 1995, *ApJS*, 98, 617  
 Truran, J. W., Arnett, D., & Cameron, A. G. W. 1967, *Canad. J. Phys.*, 45, 2315  
 Twarog, B. A. 1980, *ApJ*, 242, 242  
 Umeda, H., Nomoto, K., Kobayashi, C., Hachisu, I., & Kato, M. 1999, *ApJ*, 522, L43  
 Umeda, H., Nomoto, K., Yamaoka, H., & Wanajo, S. 1999, *ApJ*, 513, 861  
 Wheeler, J. C., Sneden, C., & Truran, J. W. 1989, *ARA&A*, 27, 279  
 Wiedenbeck, M. E., et al. 2001, *Space Sci. Rev.*, 99, 15